Electronic Supporting Information (ESI)

for

Phosphate-silica interactions in diatom biosilica and synthetic composites studied by Rotational Echo Double Resonance (REDOR) NMR spectroscopy

Felicitas Kolbe,[1] Fabian Daus,[2] Armin Geyer,[2] Eike Brunner[1]

[1] Chair Bioanalytical Chemistry, Faculty of Chemistry and Food Chemistry, TU Dresden, 01062 Dresden, Germany

[2] Department of Chemistry, Philipps-University Marburg, Hans-Meerwein-Straße 4, 35032 Marburg, Germany

1. The $^{31}P\{^{29}Si\}$ REDOR experiment

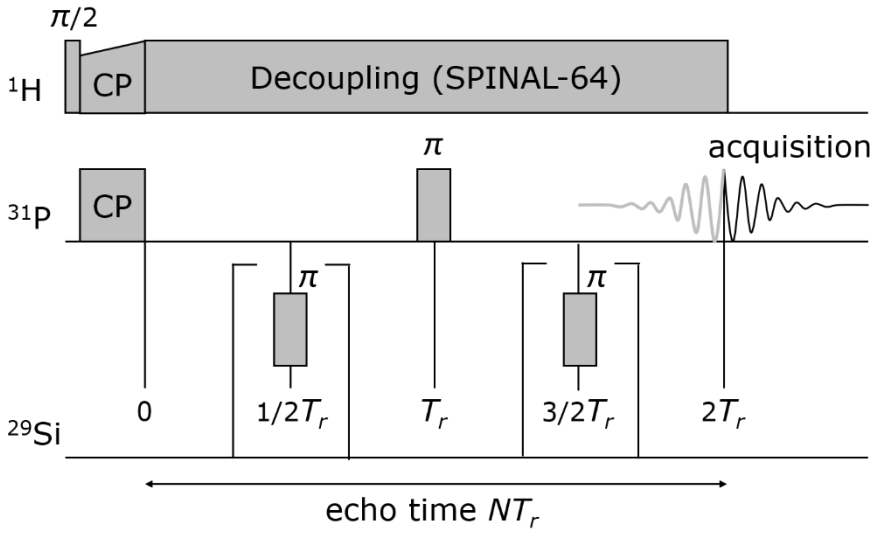

Figure S1. Pulse sequence of the ^{1}H-$^{31}P\{^{29}Si\}$ REDOR experiment. A signal intensity S_r is measured when the π-pulses on the ^{29}Si channel cause partial echo dephasing. The echo intensity S_0 is measured without ^{29}Si irradiation. The scheme is drawn for N = 2.

2. Polyallylamine-containing silica composite

2.1 Preparation

For silica precipitation in the model composite the following compounds were used: $Na_2{}^{29}SiO_3$ + NaH_2PO_4 (Merck) + PAA·HCl (polyallylamine hydrochloride, Sigma Aldrich, averaged MW 17,500 g/mol). The concentration of the used compounds can be found in Table S1. Their amounts correspond to a Si:N ratio of 1:1 and a P:N ratio of 0.43:1 which was already shown to be an optimal ratio for silica precipitation.[1,2]

Table S1. Final concentrations of the used compounds in the precipitation solution of the PAA-containing composite.

	***c* / mM**	***M* / g·mol^{-1}**
$Na_2{}^{29}SiO_3$	70	123
$NaH_2PO_4{\cdot}H_2O$	30	138
PAA·HCl	0.37	17500

For the precipitation assay, $Na_2{}^{29}SiO_3$ was dissolved in ultrapure water to receive an aqueous $Si(OH)_4$-solution. Its pH value was adjusted to 5.5±0.01 with 2.4 M HCl. NaH_2PO_4 and PAA·HCl were dissolved in ultrapure water, too. These solutions were added to the silicic acid solution and the pH was adjusted again. The precipitation solution was filled up to its final volume. After 15 min the composite was centrifuged (5 min, 2500x*g*) and washed several times. After that, the composite was dried gently at 37°C for 6 days. The dried gel was filled into MAS rotors with of 2.5 mm outer diameter.

2.2 Solid-state NMR spectroscopic and $^{31}P\{^{29}Si\}$ REDOR experiments of the PAA-containing composite

As a model system, a silica composite containing NaH_2PO_4 and polyallylamine hydrochloride was chosen in a first series of test experiments. The recorded ^{31}P CP MAS NMR spectrum shows two signals (Figure S2). The intense signal at 2.7 ppm is characteristic for phosphate groups. Interestingly, a second phosphorus signal at - 6.0 ppm appears. The assignment of this signal is not fully clear. Different possible explanations are conceivable. If these phosphate groups are in closer contact with the silica phase, a shift to lower field could occur. Another explanation is the presence of pyrophosphate in the composite, which would be consistent with the measured chemical shift. However, it could be shown, that the used NaH_2PO_4 is free of any pyrophosphate (Figure S3) and pyrophosphate formation under the applied conditions seems unlikely. Comparison with the directly excited spectrum shows a stronger CP efficiency for the signal at - 6.0 ppm than for the one at 2.7 ppm (Figure S4). Possible reasons could be either a higher number of hydrogen atoms in the neighborhood or a reduced mobility of the species compared to the phosphate causing the signal at 2.7 ppm. Both effects would cause an increase of the CP efficency.[3] Other explanations for the -6 ppm-signal would be (i) the formation of $–NH_3^+$ on the primary amines of the PAA in the slightly acidic pH or (ii) replacement of H at the phosphate. We exclude the formation of P-O-Si bonds, since the measured chemical shift is not really characteristic for such bonds[4] and the precipitation assay does not support the formation of P-O-Si bonds.

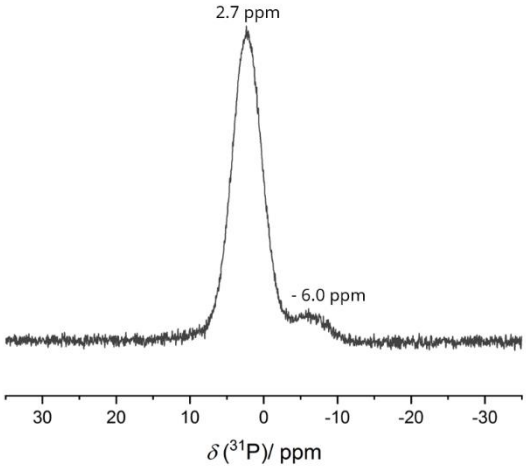

Figure S2. ^{31}P CP MAS NMR spectrum of the PAA-containing composite.

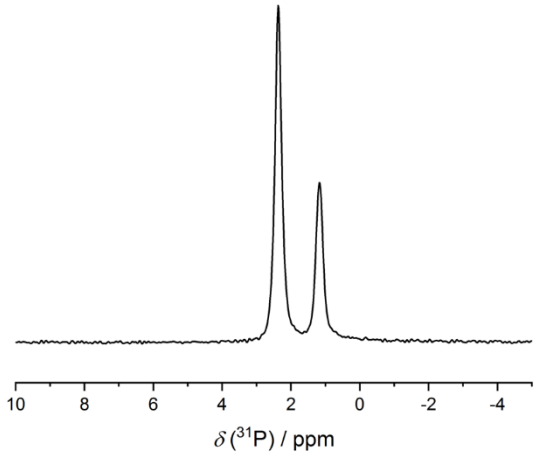

Figure S3. Directly excited ^{31}P MAS NMR spectrum of NaH_2PO_4, which was used as phosphate source in the PAA-containing composite.

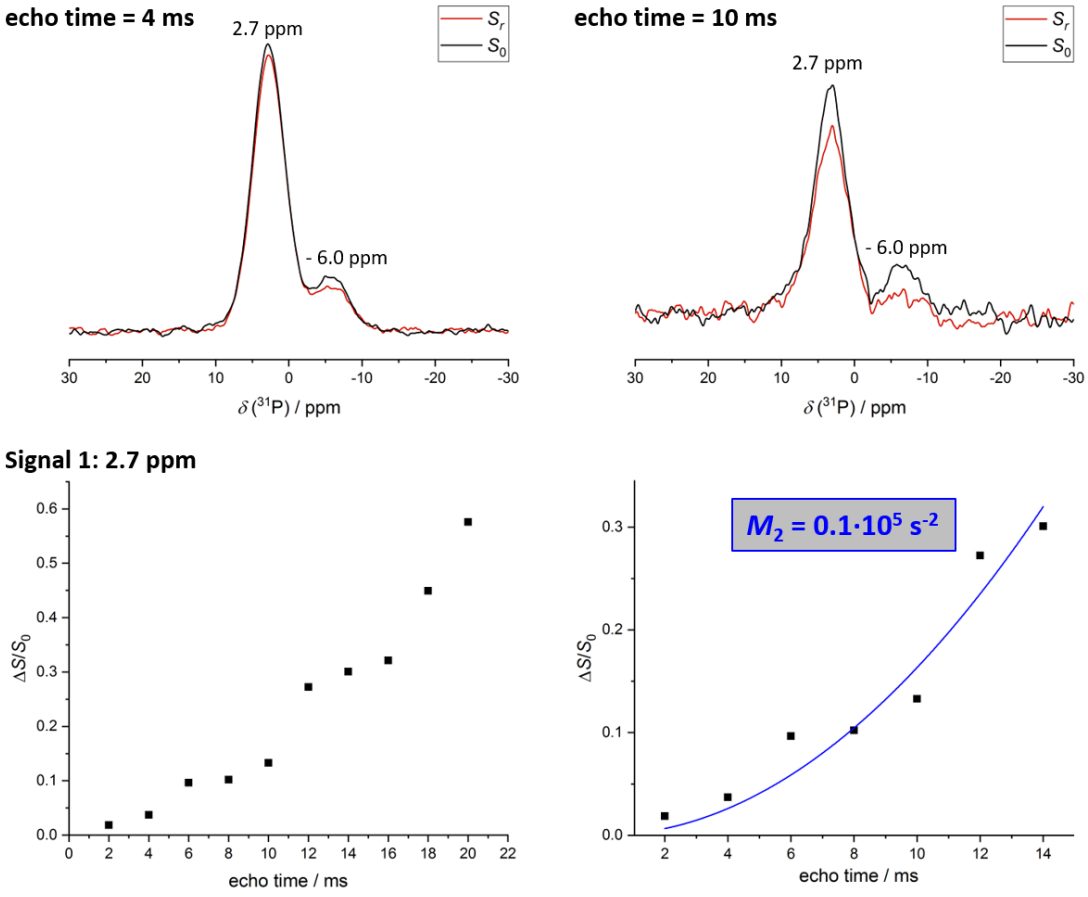

Figure S4. ^{31}P{^{29}Si} REDOR experiments of the PAA-containing composite. Top: ^{31}P spectra for two different echo times of 4 ms and 10 ms. Bottom: Experimental REDOR curve and calculation within the first order approximation.for the signal at 2.7 ppm.

The recorded $^{31}P\{^{29}Si\}$ REDOR data also allow to calculate the ^{31}P-^{29}Si second moment in the composite. Figure S4 shows ^{31}P spectra at two different echo times and the full REDOR curve for all echo times between 2 and 20 ms. At the shorter echo time of 4 ms, only minor differences between the spectra are observed but the REDOR fraction increases at 10 ms echo time. The signal at - 6.0 ppm shows a higher REDOR fraction than the signal at 2.7 ppm.

The REDOR fraction for 20 ms echo time amounts to 0.6 which means that at least 60% of the phosphate groups causing the 2.7 ppm signal are in contact with silica. The ^{31}P-^{29}Si second moment was calculated using the first order approximation and the REDOR data for echo times up to 14 ms. A relatively small value of $0.1 \cdot 10^5$ s^{-2} results which may be caused by various reasons: Phosphate could be partially embedded by the rather long PAA-chain and thus prevented from direct silica contact. It must also be taken into account that phosphate groups which do not interact with the silica, may give rise to non-dephasing signals at the same chemical shift. This would also result in an underestimation of the calculated second moment. Furthermore, the influence of mobility effects of phosphate contributing to this signal must be considered. An increased mobility of these phosphate groups in comparison to the groups at - 6.0 ppm which was also indicated by the comparison of directly excited and CP spectrum would result in a decrease of the averaged dipolar coupling constant and thus, a lower REDOR fraction compared to the signal at - 6.0 ppm.

3. Phosphopeptide/silica composites

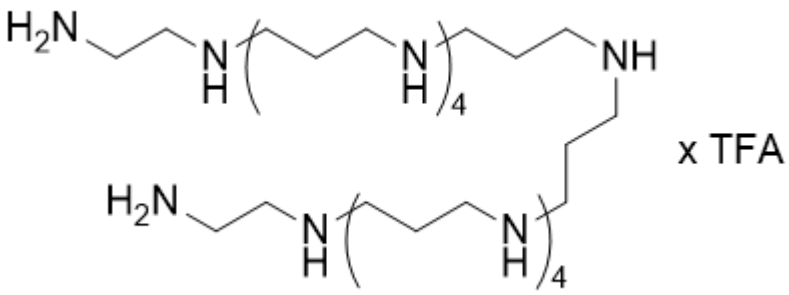

Figure S5. Structure of the synthetic LCPA used for the phosphopeptide/silica composite.

3.1 Further spectroscopic investigation

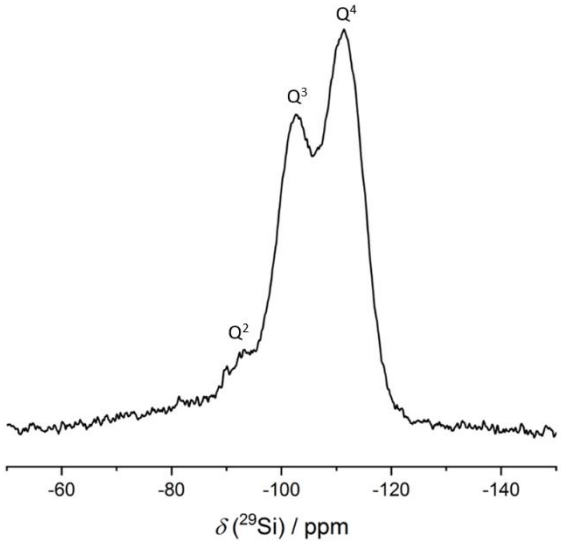

Figure S6. Directly excited ^{29}Si MAS NMR spectrum of the phosphopeptide/silica composite.

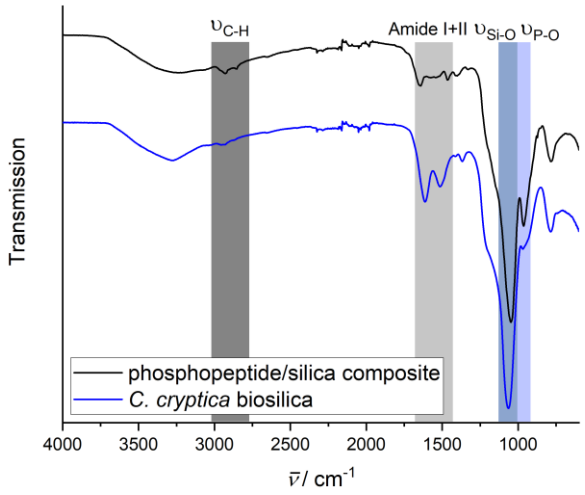

Figure S7. Attenuated Total Reflectance (ATR) InfraRed (IR) spectra of the phosphopeptide/silica composite and the *C. cryptica* biosilica. Characteristic bands proving the presence of silica, phosphate, and organic material are assigned. Note the influence of ^{29}Si isotope-labelling upon the wavenumbers of characteristic bands compared to unlabeled samples. ^{13}C- and ^{15}N-enrichment causes additional effects for the isotope-labeled biosilica.

3.2 Morphology characterization of the phosphopeptide/silica composite and biosilica

SEM images were recorded to study the morphology of the materials (Figure S8). The formation of the typical silica spheres can be observed for the precipitate. The mean diameter of these spheres seems smaller than the value of about 400 nm observed previously in precipitation studies with LCPA with an averaged chain length of 12 nitrogen atoms.[5] Possible reasons can be the different silica sources

(Na_2SiO_3 or TMOS - tetramethyl orthosilicate) or differences during preparation of the SEM samples. Moreover, a different synthetic and well-defined LCPA with a chain length of 13 nitrogen atoms was used in our study, to prevent line broadening in the NMR experiments due to structural variation of the LCPA. However, it was proven, that LCPAs are necessary for silica precipitation under mildly acidic conditions for this synthetic phosphopeptide p7-Sil01[5] as well as for the silaffins studied before.[6] Thus, the LCPA must be added to the precipitation mixture under the chosen conditions for successful silica precipitation.

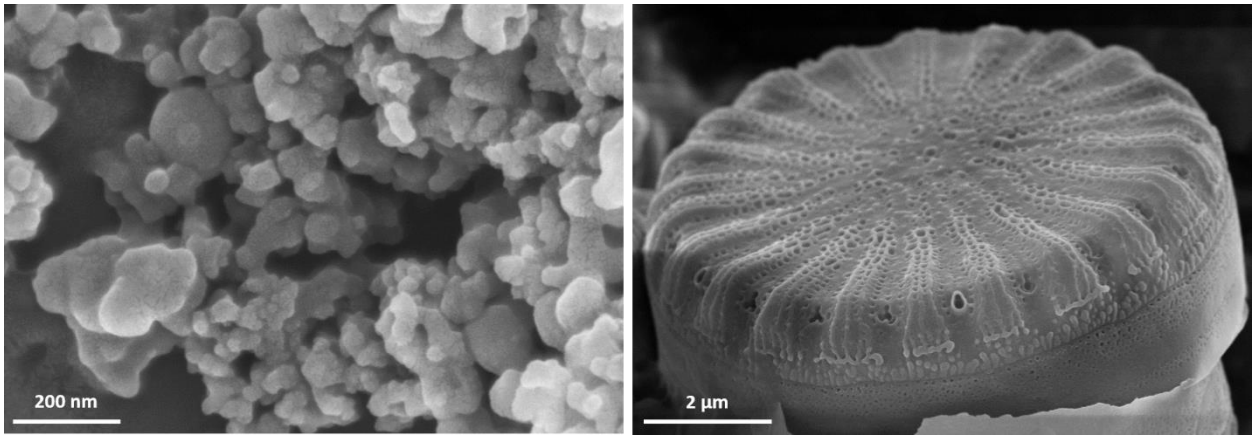

Figure S8. SEM images of the dried phosphopeptide/silica composite and the cell wall of *C. cryptica*.

3.3 Discussion of the second moment

As discussed by Bertmer *et al.*[7], the dephasing behavior in REDOR experiments within the first order approximation only depends on the heteronuclear dipolar second moment, i.e., the internuclear ^{31}P-^{29}Si distances r_i independent of the relative spatial arrangement of the different spins:

$$M_2 = \frac{4}{15}\left(\frac{\mu_0}{4\pi}\right)^2 \gamma_I^2 \gamma_S^2 \hbar^2 I(I+1) \sum_{i=1}^{n} \langle r_i^{-6} \rangle \qquad (1)$$

The term $\langle r_i^{-6} \rangle$ denotes the average value of r_i^{-6} where i is an index numbering the ^{29}Si spins surrounding the considered ^{31}P spin. The number of closely neighbored ^{29}Si nuclei is denoted by n and ħ is the Planck constant divided by 2π.The second moment further depends on the magnetic field constant μ_0 and the gyromagnetic constants γ_I *and* γ_S of ^{31}P and ^{29}Si as well as the spin quantum number I of the non-observed nucleus (^{29}Si, I = ½). For I = ½ equation 1 can be written as:

$$M_2 = \frac{1}{5}\left(\frac{\mu_0}{4\pi}\right)^2 \gamma_I^2 \gamma_S^2 \hbar^2 \sum_{i=1}^{n} \langle r_i^{-6} \rangle \qquad (2)$$

The calculation of a distance in two-spin approximation is not reasonable due to the unknown size and geometry of the spin systems in the amorphous composite material. The influence of the spin system will be discussed in the following for ^{31}P-^{29}Si distances expected under reasonable assumptions (Figure S9). Note, that we discuss equidistant spins here. Obviously, the neighborhood of one or two, maximally three ^{29}Si spins is most likely assuming distances between 4.0 and 5.0 Å. Smaller ^{31}P-^{29}Si distances are not expected, since we exclude the formation of P-O-Si bonds with a typical ^{31}P-^{29}Si distance of ca. 3.5 Å. In two-spin approximation, this would result in a second moment of $4 \cdot 10^5$ s^{-2}, much larger than the

experimentally determined value (cf. Figure S9). Instead, the REDOR experiment would yield 4.2 Å for the two-spin system. This is considerably longer than expected for covalently bound Si-O-P fragments. Thus, minimum ^{31}P-^{29}Si distances ≥ 4.2 Å are very likely. Furthermore, covalent bond formation would result in ^{31}P chemical shift between -20 ppm to -40 ppm[4] which is not observed.

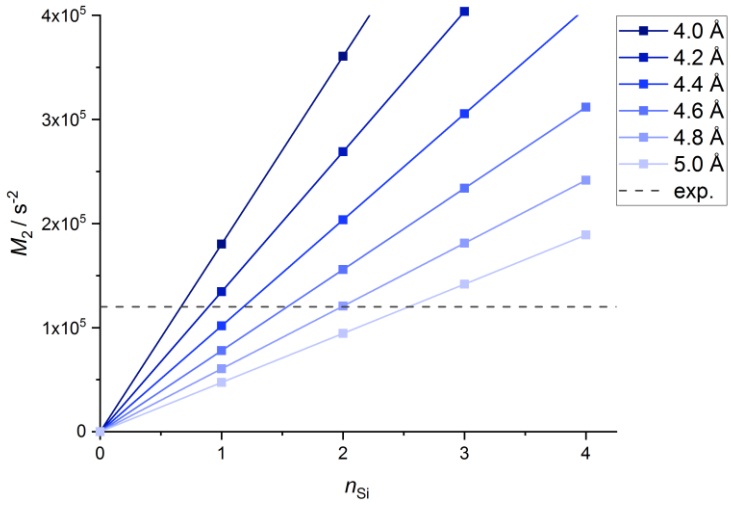

Figure S9. Second moment M_2 as a function of the averaged spin distance and the number of ^{29}Si spins in contact to the ^{31}P spin. The dashed line shows the experimental value of the second moment.

3.4 Further error discussion for the measured second moment

As already discussed, at least 80% of the phosphate are in close contact to the silica in the phosphopeptide/silica composite. Maybe even higher REDOR fractions occur at higher echo times and are only not detectable due to decreasing signal-to-noise ratio at high echo times. However, it is also possible that the missing 20% belong to phosphate groups which are not in close contact to the silica. The contribution of such phosphate groups to the overall signal intensity causes a reduced REDOR fraction and an underestimation of the second moment. In order to estimate the maximum possible error caused by this effect, we here assume that the maximum REDOR fraction of 1.0 would be reached at an echo time of 12 ms (Figure S9). We thus normalize the REDOR curve to 1.0 at 12 ms.

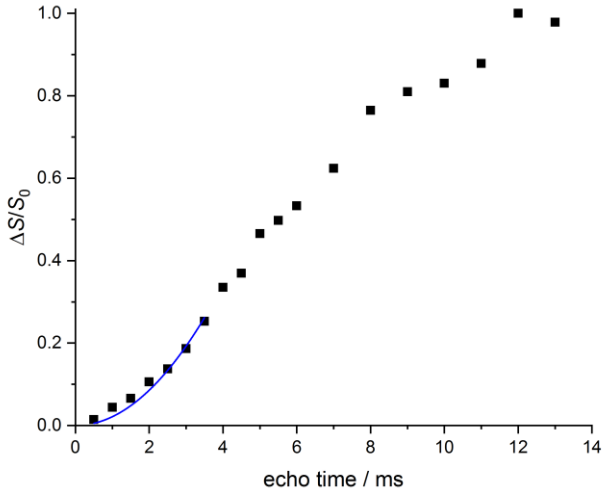

Figure S10. Normalized REDOR curve for the phosphopeptide/silica composite assuming the maximum REDOR fraction of 1.0 at an echo time of 12 ms.

Using echo times up to 3.5 ms for the first order approximation, the calculation results in a second moment of $1.6 \cdot 10^5$ s^{-2}, which is $0.4 \cdot 10^5$ s^{-2} higher than the calculated value for the silica/phosphopeptide composite using the measured REDOR fractions. This result shows that if 20% of the phosphate are not in close contact with the silica, the calculated second moment is underestimated by ca. 25%. This would not substantially influence the conclusions drawn in our manuscript.

4. References

(1) Brunner, E.; Lutz, K.; Sumper, M. Biomimetic Synthesis of Silica Nanospheres Depends on the Aggregation and Phase Separation of Polyamines in Aqueous Solution. *Phys. Chem. Chem. Phys.* **2004**, *6* (4), 854–857.

(2) Lutz, K.; Gröger, C.; Sumper, M.; Brunner, E. Biomimetic Silica Formation: Analysis of the Phosphate-Induced Self-Assembly of Polyamines. *Phys. Chem. Chem. Phys.* **2005**, *7* (14), 2812–2815.

(3) Koenig, J. L. *High-Resolution NMR Spectroscopy of Solid Polymers*; Elsevier Science, 1999.

(4) Ren, J.; Eckert, H. Superstructural Units Involving Six-Coordinated Silicon in Sodium Phosphosilicate Glasses Detected by Solid-State NMR Spectroscopy. *J. Phys. Chem. C* **2018**, *122*, 27620–27630.

(5) Daus, F.; Pfeifer, E.; Seipp, K.; Hampp, N.; Geyer, A. The Role of Phosphopeptides in the Mineralisation of Silica. *Org. Biomol. Chem.* **2020**, *18* (4), 700–706.

(6) Kröger, N.; Deutzmann, R.; Sumper, M. Polycationic Peptides from Diatom Biosilica That Direct Silica Nanosphere Formation. *Science* **1999**, *286* (5442), 1127–1132.

(7) Bertmer, M.; Züchner, L.; Chan, J. C. C.; Eckert, H. Short and Medium Range Order in Sodium Aluminoborate Glasses. 2. Site Connectivities and Cation Distributions Studied by Rotational Echo Double Resonance NMR Spectroscopy. *J. Phys. Chem. B* **2000**, *104* (28), 6541–6553.